

JOURNAL OF DIFFERENTIAL EQUATIONS 57, 172–199 (1985)

# Perturbation of a Hopf Bifurcation by an External Time-Periodic Forcing

J. M. GAMBAUDO

*Département de Mathématiques,\* Parc Valrose, 06034—Nice Cedex, France*

Received December 6, 1982; revised October 11, 1983

*Contents.* I. Introduction. II. The mathematical model. III. Dynamics of the Poincaré map in the non-resonant and weakly resonant cases. IV. Dynamics of the Poincaré map in the  $p/1$  resonant case. V. Dynamics of the Poincaré map in the  $p/2$  resonant case. VI. Dynamics of the Poincaré map in the  $p/3$  resonant case.

## I. INTRODUCTION

In this work, we develop a general study of the problem of the perturbation of an autonomous differential system in  $\mathbb{R}^2$ , by a time-periodic forcing close to a Hopf bifurcation point.

For a long time, works have been done on the problem of the perturbation of a limit cycle in the particular case of classical differential equations. An historical example is given by the forced Van der Pol oscillator [4, 5, 9].

A new interest in these problems has arisen by the development of new techniques in bifurcation theory and the help of computers. Let us cite, more particularly, some recent studies on the Van der Pol oscillator [10], on the Brusselator [14] and on the Duffing equation [7].

Previous works have not yet considered the general study of the periodic perturbation of a one parameter family of autonomous differential equations in the plane satisfying conditions for a generic Hopf bifurcation, which is what we intend to do here.

In this type of problem there are three basic parameters:

- the parameter of bifurcation,
- the amplitude of the perturbation,
- the frequency of the excitation.

This paper contains a description of the dynamics of these differential equations in this three parameter space; this approach presents the advan-

\* L.A. 168 Associé au CNRS.

tage of transforming the global problem of the perturbation of a limit cycle into a local one, which allows us to use perturbation methods.

When the ratio of the natural frequency of the bifurcating cycle to the frequency of the excitation is close to a rational number  $p/q$  (where  $p$  and  $q$  are relatively prime) resonance phenomena may occur. These phenomena are of astonishing richness when the resonance is strong (i.e., when  $q = 1, 2, 3$ ). For example, the existence of infinitely many periodic orbits will be shown in the neighborhood of the Hopf bifurcation point.

## II. THE MATHEMATICAL MODEL

### (1) *Position of the Problem, Hypotheses*

Let us consider the differential equation in  $\mathbb{R}^2$

$$\frac{du}{dt} = F(\mu, u), \quad (2.1)$$

where  $u(t) \in \mathbb{R}^2$ ,  $\mu \in \mathbb{R}$  and  $F$  is sufficiently smooth.

We assume that

$$F(\mu, 0) = 0 \quad (2.2)$$

for  $\mu$  in the neighborhood of zero and that the derivative  $D_u F(0, 0)$  has two simple eigenvalues  $\pm i\omega_0$ .

The perturbation theory in  $\mathbb{R}^2$  [15] allows us to prove the existence of eigenvalues  $\sigma(\mu)$  and  $\bar{\sigma}(\mu)$  of  $D_u F(\mu, 0)$  such that

$$\sigma(\mu) = i\omega_0 + \sigma_1\mu + \mathcal{O}(\mu^2) \quad (2.3)$$

and we assume the Hopf transversality condition

$$\operatorname{Re} \sigma_1 > 0. \quad (2.4)$$

With these assumptions, we know that we generically have a Hopf bifurcation at  $\mu = 0, u = 0$  [11].

Our goal in this paper is to study systems in  $\mathbb{R}^2$  of the form

$$\frac{du}{dt} = G(\mu, u, \varepsilon, \omega t), \quad (2.5)$$

where  $\mu$  and  $\varepsilon$  are two small real parameters,  $\omega$  is a real positive number and  $G$  satisfies the assumptions

$G$  is sufficiently smooth,

$G$  is  $2\pi$  periodic with respect to its last argument,

$G(\mu, u, 0, \omega t) = F(\mu, u)$  where  $F$  satisfies the previous hypotheses.

(2) *Normal Form*

We can rewrite (2.5) as

$$\frac{du}{dt} = F(\mu, u) + \varepsilon g(\omega t) + \varepsilon h(\mu, u, \varepsilon, \omega t), \tag{2.6}$$

where  $g(\omega t) = (\partial G/\partial \varepsilon)(0, 0, 0, \omega t)$  and  $h(\mu, u, \varepsilon, \omega t) = \mathcal{O}(\mu) + \mathcal{O}(\varepsilon) + \mathcal{O}(\|u\|)$ .

Let  $\zeta_0$  be an eigenvector of  $D_u F(0, 0)$  associated to the eigenvalue  $i\omega_0$  and  $\zeta_0^*$  the eigenvector of the adjoint operator  $[D_u F(0, 0)]^*$  associated to the eigenvalue  $-i\omega_0$  such that  $\langle \zeta_0, \zeta_0^* \rangle = 1$ .

A standard weakly non-linear change of variables [12] transforms (2.5) in

$$\frac{dz}{dt} = \sigma(\mu) z - a(\mu) |z|^2 z + \varepsilon g_1(\omega t) + l(\mu, z, \bar{z}, \varepsilon, \omega t), \tag{2.7}$$

where  $z \in \mathbb{C}$ ,  $a(\mu) \in \mathbb{C}$ ;  $l(\mu, z, \bar{z}, \varepsilon, \omega t) = \varepsilon(\mathcal{O}(\mu) + \mathcal{O}(|z|) + \mathcal{O}(\varepsilon)) + \mathcal{O}(|z|^5)$  and  $g_1(\omega t) = \langle g(\omega t), \zeta_0^* \rangle$ .

In the case  $\varepsilon = 0$ , we get the classical normal form of a Hopf bifurcation; the Hopf condition (2.4) insures that the solution  $u = 0$  is stable (resp. unstable) if  $\mu < 0$  (resp.  $\mu > 0$ ).

We assume  $\text{Re } a(0) > 0$  to have an attracting invariant circle bifurcating at the fixed point for  $\mu > 0$ , and that  $\text{Im } a(0) \geq 0$  for sake of simplicity.

(3) *Normal Forms of the Poincaré Map*

An integral form of Eq. (2.7) is

$$z(t) = e^{\sigma(\mu)t} \left[ z(0) + \int_0^t e^{-\sigma(\mu)s} (-a(\mu) |z(s)|^2 z(s) + \varepsilon g_1(\omega s) + l(\mu, z(s), \bar{z}(s), \varepsilon, \omega s)) ds \right]. \tag{2.8}$$

Solving (2.8) by a fixed point technique, we get a local expression of the Poincaré map

$$P_{\mu, \omega, \varepsilon} : \begin{cases} \mathbb{C} \rightarrow \mathbb{C} \\ z(0) \mapsto z\left(\frac{2\pi}{\omega}\right); \end{cases}$$

given by

$$P_{\mu, \omega, \varepsilon}(z) = e^{\sigma(\mu)(2\pi/\omega)} \left[ z + \frac{e^{(4\pi/\omega)\operatorname{Re}\sigma(\mu)} - 1}{2 \operatorname{Re} \sigma(\mu)} a(\mu) |z|^2 z + \varepsilon I(\mu, \omega) \right] + \tilde{I}(\mu, z, \bar{z}, \varepsilon, \omega) \tag{2.9}$$

where

$$I(\mu, \omega) = \int_0^{2\pi/\omega} e^{-\sigma(\mu)\tau} g_1(\omega\tau) d\tau$$

and (2.10)

$$\tilde{I}(\mu, z, \bar{z}, \varepsilon, \omega) = \varepsilon(\mathcal{O}(\mu) + \mathcal{O}(|z|) + \mathcal{O}(\varepsilon)) + \mathcal{O}(|z|)^5.$$

*Classical properties.* We recall that periodic cycles of the Poincaré map with rotation number  $p/q$  ( $(p, q) = 1$ ), correspond to periodic orbits of (2.5) with period  $(2\pi/q\omega)P$  and the stability types correspond.

If the Poincaré map has an invariant circle and if its restriction to this circle is isotope to the identity, then (2.5) possesses a two dimensional invariant torus.

In order to do a detailed exploration of the parameters space, we introduce a new small parameter

$$\gamma = 2\pi \left( \frac{\omega_0}{\omega} - \theta_0 \right). \tag{2.11}$$

Different situations have to be examined according to the value of  $\theta_0$ ; in each case we give, using classical techniques, the normal form of the Poincaré map.

(a) *The non-resonant case.*  $\theta_0 \notin \mathbb{Q}$ , and the weakly resonant case  $\theta_0 = p/q, q \geq 4$ . By use of the implicit function theorem and weakly non-linear change of variables, we get a canonical form for the Poincaré map

$$P_{\sigma_0, \tau_0, \rho_0}(z) = e^{2\pi i \theta_0} [z + (\sigma_0 + i\tau_0 - |z|^2) az] + \mathcal{O}(|z|^5) + \mathcal{O}(\sigma_0 |z|^3) + \mathcal{O}(\tau_0 |z|^3) + \mathcal{O}(\rho_0 |z|^3), \tag{2.12}$$

where the new real parameters  $\sigma_0, \tau_0, \rho_0$  satisfy

$$\begin{aligned} a(\sigma_0 + i\tau_0) &= \exp\left(\frac{2\pi}{\omega} \sigma(\mu) - 2i\pi\theta_0\right) - 1 + \mathcal{O}(\varepsilon) \\ &= i\gamma + \mathcal{O}(\mu) + \mathcal{O}(\varepsilon); \quad \rho_0 = \mathcal{O}(\varepsilon) \end{aligned} \tag{2.13}$$

and

$$a = \frac{a(0)}{|a(0)|} = \alpha + i\beta \quad \text{where } \alpha > 0 \text{ and } \beta \geq 0. \quad (2.14)$$

In the non-resonant case, we can pursue the development of the normal form

$$P_{\sigma_0, \tau_0, \rho_0}(z) = e^{2\pi i \theta_0} [z + (\sigma_0 + i\tau_0 - |z|^2) az] + \sum_{k=2}^p a_k |z|^{2k} z + (\mathcal{O}(\sigma_0) + \mathcal{O}(\tau_0) + \mathcal{O}(\rho_0)) |z|^3 + \mathcal{O}(|z|^{2p+2}) \quad (2.15)$$

for any integer  $p$ .

In the weakly resonant case, we find, in the normal form, a first resonant term  $\rho_0 \bar{z}^{q-1}$ .

(b) *The strongly resonant cases:*  $\theta_0 = p/q$ , where  $(p, q) = 1$  and  $q = 1, 2, 3$ . Here we have the canonical expression

$$P_{\sigma_q, \tau_q, \rho_q}(z) = e^{2\pi i (p/q)} [z + (\sigma_q + i\tau_q - |z|^2) az + \rho_q \bar{z}^{q-1}] + \mathcal{O}(\sigma_q |z|^3) + \mathcal{O}(\tau_q |z|^3) + \mathcal{O}(\rho_q |z|^q) + \mathcal{O}(|z|^5), \quad (2.16)$$

where  $q = 1, 2, 3$ .

The parameters  $(\sigma_q, \tau_q, \rho_q)$ ,  $q = 1, 2, 3$ , satisfy the same estimates (2.13) but are evidently not the same in each case.

#### (4) *Stroboscopy*

In the plane  $\varepsilon = 0$  of the parameters space  $(\mu, \gamma, \varepsilon)$ , the Poincaré map is nothing else but the stroboscopy of the differential system (2.1).

The classical theory [12] gives us the period  $T_{\mu, \gamma}$  of the bifurcating periodic orbit of the system (2.1).

*Solving the equation*

$$T_{\mu, \gamma} = \frac{2\pi}{\omega}, \quad (2.17)$$

we find easily that, in each resonant case  $\theta_0 = p/q$ , there exists in the plane  $\varepsilon = 0$  a curve

$$\gamma = f_{p/q}(\mu), \quad \mu \geq 0, \quad \text{where } f_{p/q}(0) = 0 \quad (2.18)$$

on which the Poincaré map has an invariant attracting circle of periodic points with rotation number  $p/q$ .

In the three strongly resonant cases this curve takes the form

$$\tau_q = \mathcal{O}(\sigma_q^2) \quad \text{for } q = 1, 2, 3. \quad (2.19)$$

(5) *The Resonant Terms*

The strong resonance phenomena have been the subject of detailed studies by Arnold [1]. What is new in our study is that the resonant terms appearing in the normal forms of the Poincaré map are small ( $\mathcal{O}(\rho_q)$ ), and this allows a competition between the terms  $|z|^2 z$  and  $\rho_q \bar{z}^{q-1}$  for  $q = 1, 2, 3$ .

### III. DYNAMICS OF THE POINCARÉ MAP IN THE NON-RESONANT AND WEAKLY RESONANT CASES

(1) *The Case when  $\theta_0 \neq p/4$* 

This is the standard case; the Hopf bifurcation theorem for maps states that, for  $(\sigma_0, \tau_0)$  close to zero with  $\mu > 0$ , the Poincaré map has an invariant attracting circle surrounding  $z = 0$ .

More particularly, in the resonant case  $\theta_0 = p/q$ ,  $q > 4$ , there exists a resonance horn emanating from the axis  $(\sigma_0, \tau_0) = 0$ , in which periodic orbits with rotation number  $p/q$  exist on the circle.

This resonance occurs in a region (Fig. 1) defined by

$$|\tau_0 - P_{\rho_0}(\sigma_0)| \leq K_{\rho_0} \sigma_0^{(q-2)/2} + \mathcal{O}(\rho_0 \sigma_0^{q/2}), \quad (3.1)$$

where  $P_{\rho_0}$  is a polynomial function of degree  $\leq (q-2)/2$  and  $P_{\rho_0}(0) = 0$ . The coefficients of  $P_{\rho_0}$  and  $K_{\rho_0}$  depend only on terms up to order  $q$  in the expansion of the Poincaré map [12].

(2) *The Case when  $\theta_0 = p/4$ ,  $(p, 4) = 1$* 

Here we cannot use the classical Hopf bifurcation theorem, but, as the coefficient of the resonant terms are small of order  $\mathcal{O}(\rho_0)$ , we can still prove the existence of an invariant attracting circle and of a resonance horn (in a

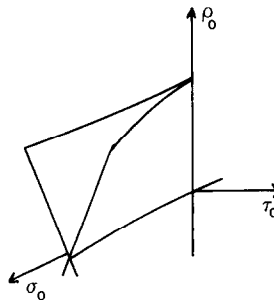


FIG. 1. A resonance horn.

region defined by (3.1)). This has been proved by Lemaire in a work on the Hopf bifurcation for maps in the case of the  $p/4$  resonance [16].

(3) *The Dynamics*

In the  $p/q$  resonance ( $q \geq 4$ ) the dynamics of such maps is well known: there is a saddle-sink pair of cycles created on the boundary of the horn by saddle-node bifurcation. In Fig. 2, we develop the phase portrait of the Poincaré map in a  $\rho_0$  constant section of the parameter space.

*Remark.* We do not distinguish, in the phase portraits, between nodes and foci because this difference does not modify the topological type of the orbit structure.

IV. DYNAMICS OF THE POINCARÉ MAP IN THE  $p/1$  RESONANT CASE

(1) *Rescaling*

The rescaling  $\tau_1 = |\sigma_1| \tau$ ,  $z = |\sigma_1|^{1/2} z'$ ,  $\rho_1 = |\sigma_1|^{3/2} \rho$  transforms the normal form (2.16) (when  $q = 1$ ) in (dropping primes)

$$\tilde{P}_{\sigma_1, \tau, \rho}(z) = z + |\sigma_1| [(\pm 1 + i\tau - |z|^2) az + \rho] + \sigma_1^2 \mathcal{O}(|z|). \tag{4.1}$$

Let us now define  $\phi_{\sigma_1, \tau, \rho}$  for  $\sigma_1 \neq 0$  by

$$|\sigma_1| (\phi_{\sigma_1, \tau, \rho} - \text{Id}) = \tilde{P}_{\sigma_1, \tau, \rho} - \text{Id}, \tag{4.2}$$

where Id denotes the identity in  $\mathbb{R}^2$  and we set

$$\phi_{0^-, \tau, \rho}(z) = z + (-1 + i\tau - |z|^2) az + \rho, \tag{4.3}$$

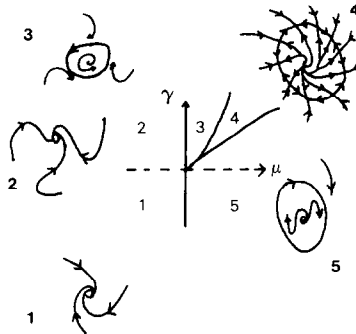


FIGURE 2

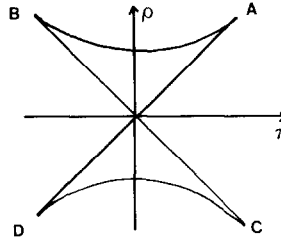


FIG. 3. The curve  $S$ .

and

$$\phi_{0^+, \tau, \rho}(z) = z + (1 + i\tau - |z|^2)az + \rho. \tag{4.4}$$

(2) *Fixed Points of  $\tilde{P}_{\sigma_1, \tau, \rho}$*

We recall briefly the

DEFINITION. A fixed point  $P$  of a diffeomorphism  $\phi$  is called singular if 1 is an eigenvalue of  $D\phi(P)$ . A non-singular fixed point is called regular.

Then we have the immediate (but useful)

LEMMA 4.1. Assume that the small parameter  $\sigma_1$  is different from zero, then:  $z_0$  is a fixed point of  $\tilde{P}_{\sigma_1, \tau, \rho}$  iff  $z_0$  is a fixed point of  $\phi_{\sigma_1, \tau, \rho}$ . The saddle (resp. singular) fixed points of  $\phi_{\sigma_1, \tau, \rho}$  are saddle (resp. singular) fixed points of  $\tilde{P}_{\sigma_1, \tau, \rho}$ .

Concerning the asymptotic behavior ( $\sigma_1 \rightarrow 0$ ) we have the following:

- LEMMA 4.2. (1)  $\phi_{0^-, \tau, \rho}$  has only one (regular) fixed point.  
 (2) Let  $S = \{(\tau, \rho) \in \mathbb{R}^2, 3\tau^2 \leq 1, \rho^2 = [2(1 + 9\tau^2) \pm (1 - 3\tau^2)^{3/2}]/27\}$ .  
 (a) Outside  $S$ ,  $\phi_{0^+, \tau, \rho}$  has only one (regular) fixed point.  
 (b) Inside  $S$ ,  $\phi_{0^+, \tau, \rho}$  has three (regular) fixed points.  
 (c) On the curve  $S$

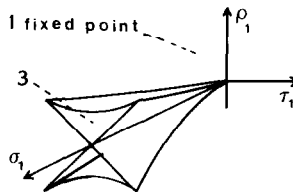


FIG. 4. Situation in the  $(\sigma_1, \tau_1, \rho_1)$  space.



( $\alpha$ ) If  $(\tau, \rho)$  is different from  $0 = (0, 0)$ ,

$$A = \left( \frac{1}{\sqrt{3}}, \frac{2}{3} \sqrt{\frac{2}{3}} \right), \quad B = \left( -\frac{1}{\sqrt{3}}, \frac{2}{3} \sqrt{\frac{2}{3}} \right),$$

$C = -B$  and  $D = -A$ , then  $\phi_{0^+, \tau, \rho}$  has one regular and one singular fixed points

( $\beta$ ) If  $(\tau, \rho) = A, B, C$  or  $D$ ,  $\phi_{0^+, \tau, \rho}$  has only one (singular) fixed point.

( $\gamma$ ) If  $(\tau, \rho) = (0, 0)$ ,  $\phi_{0^+, \tau, \rho}$  has one regular fixed point  $z = 0$  and the circle of radius 1 is fixed.

(3) We have a saddle fixed point (and only one) exclusively in the case 2b.

*Proof.* (1) If  $z_0$  is a fixed point of  $\phi_{0^-, \tau, \rho}$ , then the following equation is satisfied

$$\xi^3 + 2\xi^2 + (1 + \tau^2)\xi - \rho^2 = 0 \quad \text{where } \xi = |z_0|^2. \quad (4.5)$$

Equation (4.5) has only one positive root and the fixed point is given by

$$z_0 = \frac{-\rho}{a(-1 + i\tau - \xi)}. \quad (4.6)$$

Looking at  $D\phi_{0^-, \tau, \rho}(z_0)$  we verify easily that the eigenvalues are complex conjugate and not real.

(2) If  $z_0$  is a fixed point of  $\phi_{0^+, \tau, \rho}$ , then we have

$$\xi^3 - 2\xi^2 + (1 + \tau^2)\xi - \rho^2 = 0 \quad \text{where } \xi = |z_0|^2. \quad (4.7)$$

Solving for the zeros of (4.7) we find two coincident roots on the curves (defined in Lemma 4.2). At the cusps  $A, B, C$  and  $D$  the three roots coincide (Fig. 5). Let  $\xi$  be a real root of (4.7) and  $(\tau, \rho, \xi) \neq (0, 0, 1)$  then the corresponding fixed point is given by

$$z_0 = \frac{-\rho}{a(1 + i\tau - \xi)}. \quad (4.8)$$

(If  $(\tau, \rho) = 0$ , the lemma is obvious.)

1 is an eigenvalue of  $D\phi_{0^+, \tau, \rho}(z_0)$  iff

$$3\xi^2 - 4\xi + 1 + \tau^2 = 0 \quad (4.9)$$

and the compatibility of Eqs. (4.7) and (4.9) is realized on the curve  $S$ .

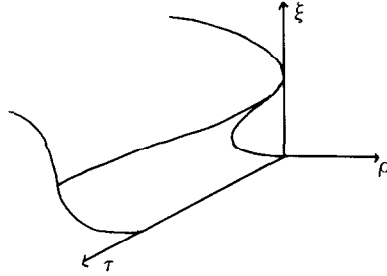


FIG. 5. The solution of Equation (4.7).

(3) Results also from a quite simple study of the eigenvalues of  $D\phi_{0^-, \tau, \rho}(z_0)$  and  $D\phi_{0^+, \tau, \rho}(z_0)$ .

Now, we can establish a similar result for the full Poincaré map  $\tilde{P}_{\sigma_1, \tau, \rho}$ .

**PROPOSITION 4.1.** (1) *Let  $\tau, \rho \in \mathbb{R}^2$  and  $\sigma_1 < 0$  be sufficiently small then  $\tilde{P}_{\sigma_1, \tau, \rho}$  has only one (regular) fixed point.*

(2) *For  $\sigma_1 > 0$  sufficiently small, there exists in the  $(\tau, \rho)$  space a closed curve  $S_{\sigma_1}(\mathcal{C}(\sigma_1))$  close to  $S$  (Fig. 6)) smooth excepted in five points; a double point  $0_{\sigma_1}$  (on the line  $\rho = 0$ ) and four cusps  $A_{\sigma_1}, B_{\sigma_1}, C_{\sigma_1}$  and  $D_{\sigma_1}$ , respectively  $\mathcal{C}(\sigma_1)$  close to  $A, B, C$  and  $D$ , such that:*

- (a) *outside  $S_{\sigma_1}$ ,  $\tilde{P}_{\sigma_1, \tau, \rho}$  has only one (regular) fixed point,*
- (b) *inside  $S_{\sigma_1}$ ,  $\tilde{P}_{\sigma_1, \tau, \rho}$  has three (regular) fixed points,*
- (c) *on the curve  $S_{\sigma_1}$*

( $\alpha$ ) *if  $(\tau, \rho)$  is different from  $0_{\sigma_1}, A_{\sigma_1}, B_{\sigma_1}, C_{\sigma_1}$  and  $D_{\sigma_1}$ , then  $\tilde{P}_{\sigma_1, \tau, \rho}$  has one regular and one singular fixed point (a saddle node bifurcation occurs on  $S_{\sigma_1}$ ),*

( $\beta$ ) *if  $(\tau, \rho) = A_{\sigma_1}, B_{\sigma_1}, C_{\sigma_1}$  or  $D_{\sigma_1}$ ,  $\tilde{P}_{\sigma_1, \tau, \rho}$  has only one (singular) fixed point.*

( $\gamma$ ) *If  $(\tau, \rho) = 0_{\sigma_1}$ ,  $\tilde{P}_{\sigma_1, \tau, \rho}$  has one regular fixed point  $z = 0$  and a closed fixed curve.*

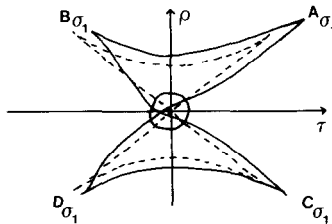


FIG. 6. The curves  $S$  and  $S_{\sigma_1}$ .

(3) We have a saddle fixed point (and only one) exclusively in the case 2b.

*Proof.* Using classical perturbation methods (implicit function theorem) and Lemmas 4.1 and 4.2 we easily prove this proposition excepted in the case  $\sigma_1 > 0$ , in an arbitrary small neighborhood  $\mathcal{V}$  of  $(\tau, \rho) = 0$ .

This is due to the fact that a fixed circle (for the map  $\phi_{0^+,0,0}$ ) is a very non-generic property.

In order to achieve the proof of Proposition 4.1 and to have a more complete description of the dynamics of  $\tilde{P}_{\sigma_1, \tau, \rho}$  in  $\mathcal{V}$  we give the

**PROPOSITION 4.2.** (1) *There exists a neighborhood  $\mathcal{V}$  of  $(0, 0)$  in the  $(\tau, \rho)$  space such that, if  $\sigma_1 > 0$  is sufficiently small,  $\tilde{P}_{\sigma_1, \tau, \rho}$  has an invariant attracting closed curve  $(\mathcal{O}(\sigma_1))$  close to the circle of center  $z = 0$  and radius 1).*

(2) *For  $\sigma_1 > 0$  sufficiently small, there exist in  $\mathcal{V}$  two curves*

$$\begin{aligned} \rho_1(\tau) &= (1 + \mathcal{O}(\sigma_1^{1/8}))(\tau - u_{\sigma_1}), \\ \rho_2(\tau) &= -(1 + \mathcal{O}(\sigma_1^{1/8}))(\tau - u_{\sigma_1}) \quad \text{where } 0_{\sigma_1} = (u_{\sigma_1}, 0) \end{aligned}$$

such that

— if  $(\rho - \rho_2(\tau))(\rho - \rho_1(\tau)) < 0$ , the invariant curve of  $\tilde{P}_{\sigma_1, \tau, \rho}$  has two hyperbolic fixed points (a saddle and a sink),

— if  $(\rho - \rho_2(\tau))(\rho - \rho_1(\tau)) > 0$  it has no fixed point,

— on the two curves a saddle-node bifurcation occurs,

— at  $\mathcal{O}_{\sigma_1}$  the invariant curve is fixed.

*Proof.* (1) Let us do the new rescaling  $\tau = \sigma_1^{1/4}t$ ,  $\rho = \sigma_1^{1/4}r$ , the change of variables

$$z = (1 + \sigma_1^{3/16}x) e^{i\theta} \tag{4.10}$$

transforms  $\tilde{P}_{\sigma_1, \sigma_1^{1/4}t, \sigma_1^{1/4}r}$  in

$$\begin{aligned} X &= (1 - 2\alpha\sigma_1)x + \mathcal{O}(\sigma_1^{17/16}), \\ \Theta &= \theta + \mathcal{O}(\sigma_1^{7/16}). \end{aligned} \tag{4.11}$$

The map is now in the standard Ruelle–Takens form [17], and this provides the first part of the proposition.

(2) In fact (4.11) can be detailed as follows:

$$X = (1 - 2\alpha\sigma_1)x - \beta\sigma_1^{17/16}t + \cos\theta\sigma_1^{17/16}r + \mathcal{O}(\sigma_1^{19/16}), \tag{4.12}$$

$$\Theta = \theta + \sigma_1^{5/4}(\alpha t - r \sin\theta) - 2\beta x^{19/16} + \mathcal{O}(\sigma_1^{22/16}). \tag{4.13}$$

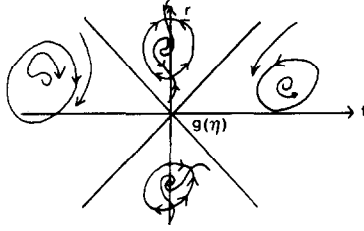


FIGURE 7

Precising  $x$  at the order  $\sigma_1^{1/16}$  leads to a more precise expression of the diffeomorphism on the invariant circle

$$\theta \mapsto \Theta = \theta + \frac{\sigma_1^{5/4}}{\alpha} (t - r(\alpha \sin \theta + \beta \cos \theta)) + \mathcal{O}(\sigma_1^{1/8}). \quad (4.14)$$

Now, we can use the non-generic property of the persistence of a fixed curve (described in Section II.4) at the point  $0_{\sigma_1} = (u_{\sigma_1}, 0) \in \mathcal{V}$  in the  $(\tau, \rho)$  space; it follows that (4.14) can be rewritten as

$$\begin{aligned} \Theta = \theta + \frac{\eta^{10}}{\alpha} (t - g(\eta))(1 + g_1(\eta, t, r, \theta)) \\ - r(\alpha \sin \theta + \beta \cos \theta + g_2(\eta, t, r, \theta)), \end{aligned} \quad (4.15)$$

where  $\eta = \sigma_1^{1/8}$ ,  $\sigma_1^{1/4} g(\eta) = u_{\sigma_1}$  and  $g_1$  and  $g_2$  are  $\mathcal{O}(\eta)$ .

The second part of the proposition results from an immediate application of the implicit function theorem to the fixed points equation of (4.15). (The dynamics of the Poincaré map in the  $(t, r)$  plane is represented in Fig. 7.)

This achieves the proof of Proposition 4.2 and consequently of Proposition 4.1.

(3) *Sinks and Sources, Hopf Bifurcation*

Now we establish results concerning the stability of the fixed points of  $\tilde{P}_{\sigma_1, \tau, \rho}$ .

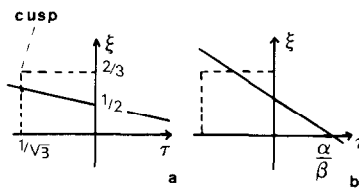


FIG. 8. (a)  $\beta/\alpha < 1/\sqrt{3}$ , (b)  $\beta/\alpha > 1/\sqrt{3}$ .

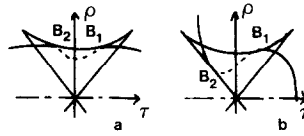


FIG. 9. (a)  $\beta/\alpha < 1/\sqrt{3}$ , (b)  $\beta/\alpha > 1/\sqrt{3}$ .

Routine calculations yield the

LEMMA 4.3. (1)  $\phi_{0^-, \tau, \rho}$  has a fixed point  $z_0$  such that trace  $D\phi_{0^-, \tau, \rho}(z_0) = 2$  iff  $\beta \neq 0$  and  $(\tau, \rho)$  belongs to the  $\xi$  parametrized curve  $H^-$  defined by

$$\tau = -\frac{\alpha}{\beta} (1 + 2\xi),$$

$$\rho = \pm \frac{1}{\beta} (\xi^3 + 2\xi^2 + (1 + \tau^2) \xi)^{1/2}, \quad \text{where } \xi \geq 0. \quad (4.16)$$

(2)  $\phi_{0^+, \tau, \rho}$  has a fixed point  $z_0$  such that trace  $D\phi_{0^+, \tau, \rho}(z_0) = 2$  iff  $(\tau, \rho)$  belongs to the  $\xi$  parametrized curve  $H^+$  defined by

$$\xi^3 - 2\xi^2 + (1 + \tau^2) \xi - \rho^2 = 0,$$

$$\alpha - \beta\tau - 2\alpha\xi = 0, \quad \text{where } \xi \geq 0. \quad (4.17)$$

The system (4.17) can be seen in the  $(\tau, \rho, \xi)$  space as the intersection of the plane  $\alpha - \beta\tau - 2\alpha\xi = 0$  with the surface described in Fig. 5. This intersection can be of two different types according to the value of the ratio  $\beta/\alpha$ . Projections of these two types are represented in Figs. 8 and 9. The intersection of  $H^+$  and  $S$  can be transversal or tangential (Fig. 10). The tangential intersections occur at four points in the  $(\tau, \rho)$  space:

$$B_1 = (\bar{\tau}, (\bar{\xi}^3 - 2\bar{\xi}^2 + (1 + \bar{\tau}^2) \bar{\xi})^{1/2}),$$

$$B_2 = (\bar{\tau}, (\bar{\xi}^3 - 2\bar{\xi}^2 + (1 + \bar{\tau}^2) \bar{\xi})^{1/2}),$$

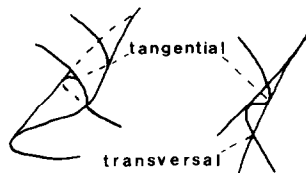


FIGURE 10

and their corresponding symmetric points  $B_3$  and  $B_4$  where  $(\bar{\tau}, \bar{\xi}) = (\alpha/(\beta + 2), 1/(2 - \beta))$  and  $(\tilde{\tau}, \tilde{\xi}) = (\alpha/(\beta - 2), 1/(2 - \beta))$ .

We have the

PROPOSITION 4.3. (1) Let  $\sigma_1 < 0$  be sufficiently small, a Hopf bifurcation occurs for  $\tilde{P}_{\sigma_1, \tau, \rho}$  iff  $(\tau, \rho)$  belongs to a smooth curve  $H_{\sigma_1}^-, \mathcal{O}(\sigma_1)$  close to  $H^-$  (Fig. 11).

(2) Let  $\sigma_1 > 0$  be sufficiently small,  $\tilde{P}_{\sigma_1, \tau, \rho}$  possesses a conservative fixed point (see definition below) iff  $(\tau, \rho)$  belongs to a smooth curve  $H_{\sigma_1}^+, \mathcal{O}(\sigma_1)$  close to  $H^+$ , which has a tangential intersection with  $S_{\sigma_1}$  at four points  $B_{1, \sigma_1}, B_{2, \sigma_1}, B_{3, \sigma_1}, B_{4, \sigma_1}$  resp.  $\mathcal{O}(\sigma_1)$  close to  $B_1, B_2, B_3$  and  $B_4$ .

— If  $(\tau, \rho)$  is on one of the two curvilinear segments  $\widehat{B_{1, \sigma_1}, B_{2, \sigma_1}}$  or  $\widehat{B_{3, \sigma_1}, B_{4, \sigma_1}}$  of  $H_{\sigma_1}^+, \tilde{P}_{\sigma_1, \tau, \rho}$  possesses a conservative saddle point.

— If not,  $\tilde{P}_{\sigma_1, \tau, \rho}$  possesses a Hopf bifurcation point.

Proof. A regular fixed point  $z_0$  such that  $\text{Det } D\tilde{P}_{\sigma_1, \tau, \rho}(z_0) = 1$  is either a conservative fixed point or a Hopf bifurcation point.

It is easy to see that  $\phi_{0^+, \tau, \rho}$  possesses a saddle point  $z_0$  such that  $\text{trace } D\phi_{0^+, \tau, \rho}(z_0) = 2$  iff  $(\tau, \rho)$  belongs to one of the two curvilinear segments  $\widehat{B_1 B_2}$  and  $\widehat{B_3 B_4}$  on  $H^+$ .

We remark that

$$\text{Det } D\tilde{P}_{\sigma_1, \tau, \rho}(z_0) = 1 + |\sigma_1| (\text{trace } D\phi_{0^\pm, \tau, \rho}(z_0) - 2) + \mathcal{O}(\sigma_1^2). \tag{4.18}$$

Then the proof of Proposition 4.3 results directly from perturbation calculations.

The points  $B_{i, \sigma_1}$  correspond to fixed points of  $\tilde{P}_{\sigma_1, \tau, \rho}$  where 1 is a double non-semi-simple eigenvalue of the derivative.

We are now able to describe the Hopf and saddle-node bifurcations set and the stability of the fixed points for small values of  $\sigma_1$ .

For sake of simplicity, we represent, in Figs. 12a and b,  $S_{\sigma_1}$  and  $H_{\sigma_1}^+$  by their asymptotic limits  $S$  and  $H^+$ .

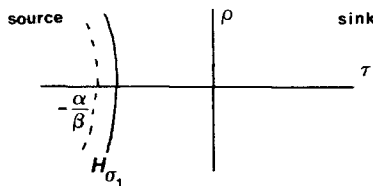


FIG. 11.  $\sigma_1 < 0$ .

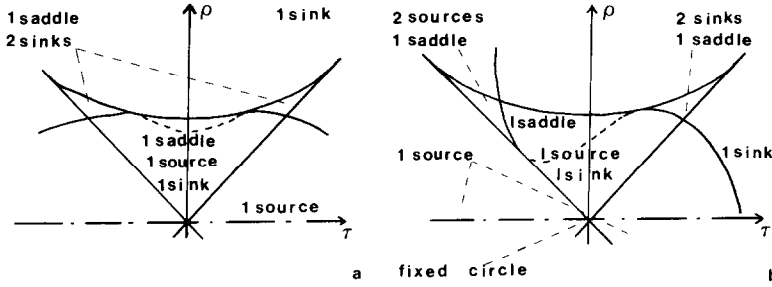


FIG. 12.  $\sigma_1 > 0$ , (a)  $\beta/\alpha < 1/\sqrt{3}$ , (b)  $\beta/\alpha > 1/\sqrt{3}$ . The dotted line corresponds to a conservative saddle point.

(4) Homoclinic Points

We detail here the situation in the neighborhood of the points  $B_{i,\sigma_1}$ .

(a) Normal form. Let  $B_{i,\sigma_1} = (\bar{\tau}_{\sigma_1}, \bar{\rho}_{\sigma_1})$  and  $\sigma_1 > 0$  be fixed and small.

Using normal forms techniques we give an expression of the Poincaré map for  $(\tau, \rho)$  close to  $B_{i,\sigma_1}$  and  $z$  close to the corresponding singular fixed point

$$\begin{aligned} X_1 &= x_1 + \sigma_1(-y_1 + \mu_1 x_1 + bx_1^2) + \sigma_1(\mathcal{O}(\|\mu\|^3)) + \mathcal{O}((x_1, y_1)^3), \\ Y_1 &= y_1 + \sigma_1(\mu_2 + x_1^2) + \sigma_1(\mathcal{O}(\|\mu\|^3)) + \mathcal{O}((x_1, y_1)^3), \end{aligned} \tag{4.19}$$

where  $\mu_1$  and  $\mu_2$  are  $\mathcal{O}(\tau - \bar{\tau}_{\sigma_1}) + \mathcal{O}(\rho - \bar{\rho}_{\sigma_1})$ .

The rescaling:  $x_1 = \varepsilon_1^2 x$ ,  $y_1 = \varepsilon_1^3 y$ ,  $\mu_1 = \varepsilon_1 \varepsilon_2$ ,  $\mu_2 = -\varepsilon_1^4$  transforms (4.19) in

$$\begin{aligned} X &= x + \sigma_1 \varepsilon_1(-y) + b\sigma_1 \varepsilon_1^2 x^2 + \sigma_1 \varepsilon_1 \mu_1 x + \sigma_1 \mathcal{O}(\varepsilon_1^4), \\ Y &= y + \sigma_1 \varepsilon_1(x^2 - 1) + \sigma_1 \mathcal{O}(\varepsilon_1^4). \end{aligned} \tag{4.20}$$

We set  $\tau = \sigma_1 \varepsilon_1$ , then (4.20) can be rewritten as

$$\begin{aligned} (X, Y) &= \phi_\tau(x, y) + \tau(\varepsilon_1 g_1(x, y, \sigma_1, \varepsilon_1, \varepsilon_2) \\ &\quad + \varepsilon_2 g_2(x, y, \sigma_1, \varepsilon_1, \varepsilon_2)), \end{aligned} \tag{4.21}$$

where

$$g_1(x, y, \sigma_1, 0, 0) = (bx^2, 0), \quad g_2(x, y, \sigma_1, 0, 0) = (x, 0)$$

and  $\phi_\tau$  is the “time  $\tau$ ” map of the Hamiltonian system defined by

$$H_1(x, y) = -x + \frac{x^3}{3} + \frac{y^2}{2} \tag{4.22}$$

and represented in Fig. 13.

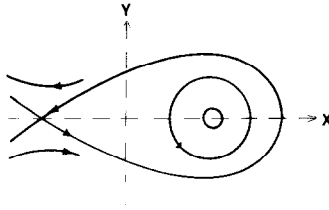


FIGURE 13

(b) *General results.* Recent works have been done on the study of systems of the form

$$\phi_{\tau, \varepsilon_1, \varepsilon_2}(x) = \phi_\tau(x) + \tau(\varepsilon_1 g_1(x, \varepsilon_1, \varepsilon_2) + \varepsilon_2 g_2(x, \varepsilon_1, \varepsilon_2)), \tag{4.23}$$

where  $x \in \mathbb{R}^2$ ,  $\phi_\tau$  is the “time  $\tau$ ” map of a Hamiltonian system

$$\frac{dx}{dt} = F(x), \tag{4.24}$$

$(\varepsilon_1, \varepsilon_2)$  is a small parameter and  $\tau$  bounded and independent of  $\varepsilon_1$  and  $\varepsilon_2$ . For small values of  $\tau$ , Iooss [13] has solved the problem of the existence of a smooth invariant circle for  $\phi_{\tau, \varepsilon_1, \varepsilon_2}$  even “far” from the Hopf bifurcation which occurs in moving parameters as  $\varepsilon_j$ .

In [8], we have proved the following result concerning homoclinic or heteroclinic points:

**THEOREM 4.1.** *Assume that the system (4.24) possesses an homoclinic (resp. heteroclinic) orbit  $q^0(t)$  and that*

$$\begin{aligned} &(M_1(\tau, t_0), M_2(\tau, t_0)) \neq (0, 0) \quad \text{for } t_0 \in [0, \tau[ \\ &\text{where } M_i(\tau, t_0) = \sum_{-\infty}^{+\infty} \text{Det} (f(q^0((n+1)\tau + t_0), \\ &\quad g_i(q^0(n\tau + t_0), 0, 0)). \end{aligned} \tag{4.25}$$

*Then, there exists a neighborhood  $\mathcal{V}$  of  $(0, 0)$  in the  $(\varepsilon_1, \varepsilon_2)$  plane (independent of  $\tau$ ) such that, for  $\tau$  fixed, the family of points  $(u, t_u) \in \mathbb{R}^{2*} \times [0, \tau[$  satisfying  $u \cdot M(\tau, t_u) = 0$ , corresponds to a family of curves  $f_u(\varepsilon_1, \varepsilon_2) = 0$  in  $\mathcal{V}$ , tangent to  $u$  at  $(0, 0)$ , on which  $\phi_{\tau, \varepsilon_1, \varepsilon_2}$  has a set of homoclinic (resp. heteroclinic) points. Inside the envelope of this family of curves,  $\phi_{\tau, \varepsilon_1, \varepsilon_2}$  possesses transverse homoclinic (resp. heteroclinic) points.*

In our case (4.21), the condition (4.25) is satisfied; indeed, when  $\tau \rightarrow 0$ ,





FIGURE 14

$M_i(\tau, t_0) \rightarrow \int_{\text{int } \phi^0(t)} \text{Div } g_i(x, 0, 0) dx = I_i$  and  $I_2 = \int_{\text{int } \phi^0(t)} dx \neq 0$ . Then, for  $\tau$  sufficiently small (and this is the case in (4.21)),  $M_2(\tau, t_0) \neq 0 \forall t_0 \in [0, \tau[$ .

In (4.21) the three parameters are dependent, and we only study (4.23) in the plane  $\tau = \sigma_1 \varepsilon_1$  of the  $(\tau, \varepsilon_1, \varepsilon_2)$  space; this plane crosses necessarily the region where  $\phi_{\tau, \varepsilon_1, \varepsilon_2}$  possesses transverse homoclinic points. It results that  $\tilde{P}_{\sigma_1, \tau, \rho}$  possesses a horn of homoclinic points emanating from  $B_{i, \sigma_1}$  in the  $(\tau, \rho)$  space (Fig. 14). Coming back to the initial system (2.5) and using Smale homoclinic theorem [18] we have then proved the

**COROLLARY 4.2.**  $\forall \mathcal{V}$ , neighborhood of  $(0, 0)$  in  $\mathbb{R}^2, \forall V$ , neighborhood of  $(0, 0, 0)$  in  $\mathbb{R}^3, \forall n \in \mathbb{N}^*, \exists V_n \subset V$ , an open set, such that, for  $(\mu, \varepsilon, \omega)$  satisfying  $(\mu, \varepsilon, \omega_0/\omega - n) \in V_n$ , (2.5) generically possesses infinitely many periodic and homoclinic orbits in  $\mathcal{V}$ .

In the following section, we give numerical results concerning an averaging of the Poincaré map which allows us to understand the way the phase portraits vary with the parameters.

(5) *Averaging and Phase Portrait, Computer Assisted Study*

Following Arnold [1], we consider the phase portrait of the differential equations which “approach”<sup>1</sup> the map  $\tilde{P}_{\sigma_1, \tau, \rho}$ :

$$\text{If } \sigma_1 < 0, \quad \frac{dz}{dt} = (-1 + i\tau - |z|^2) az + \rho. \tag{4.26}$$

$$\text{If } \sigma_1 > 0, \quad \frac{dz}{dt} = (1 + i\tau - |z|^2) az + \rho. \tag{4.27}$$

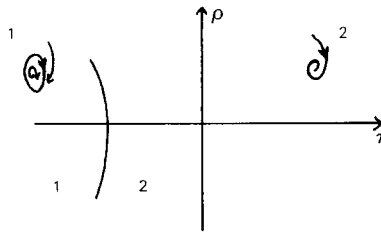


FIG. 15. Phase portrait of Equation (4.26).

<sup>1</sup> It means that the “time  $\sigma_1$  map” of these equations is  $\mathcal{O}(\sigma_1^2)$  close to  $\tilde{P}_{\sigma_1, \tau, \rho}$ .

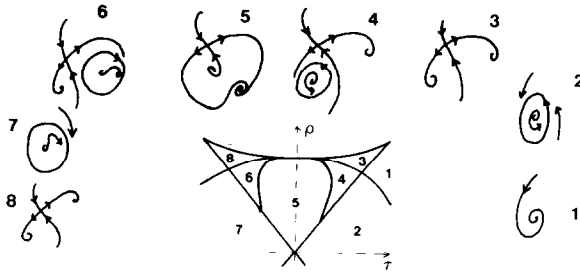


FIG. 16. Phase portrait of Equation (4.27); the case  $\beta/\alpha < 1/\sqrt{3}$ .

In addition to the previous types of bifurcation we have described (saddle-node and Hopf), a computer assisted study shows that new types of bifurcation may occur: homoclinisation and saddle-node of invariant circles [6]. The phase portraits are described in Figs. 15–17.

*Remark.* Around  $B_i$  for  $i = 1, 2, 3, 4$ , in the case of the Poincaré map, we have proved the existence of homoclinic points; in the case of ODE, a complete study has been done by Bogdanov [2].

### V. DYNAMICS OF THE POINCARÉ MAP IN THE $P/2$ RESONANT CASE

The dynamics of the Poincaré map is best understood if one looks at its second iterate:

$$P_{\sigma_2, \tau_2, \rho_2}^2(z) = z + 2(\sigma_2 + i\tau_2 - |z|^2)az + 2\rho_2\bar{z} + \mathcal{O}(\sigma_2|z|^3) + \mathcal{O}(\tau_2|z|^3) + \mathcal{O}(\rho_2|z|^2) + \mathcal{O}(|z|^5). \quad (5.1)$$

The fixed points of  $\tilde{P}_{\sigma_2, \tau_2, \rho_2}^2$  different from zero correspond to periodic points with period two of the Poincaré map.

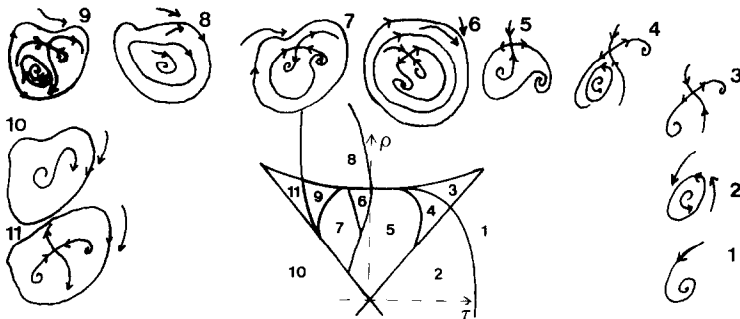


FIG. 17. Phase portrait of Equation (4.27); the case  $\beta/\alpha > 1/\sqrt{3}$ .

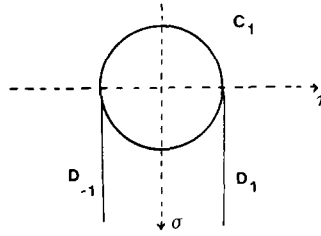


FIGURE 18

By changing  $z$  in  $iz$  we can reduce our study to the case  $\rho_2 \geq 0$ .

(1) *The Rescaling*

The rescaling  $z = \rho_2^{1/2} z'$ ;  $\sigma_2 + i\tau_2 = \rho_2(\sigma + i\tau)$  yields the equation (dropping primes)

$$\tilde{P}_{\sigma,\tau,\rho_2}^2(z) = z + 2\rho_2[(\sigma + i\tau - |z|^2)az + \bar{z}] + \mathcal{O}(\rho_2^{3/2}|z|^2). \tag{5.2}$$

For  $\rho_2 \neq 0$ , we define  $\psi_{\sigma,\tau,\rho_2}$  by

$$2\rho_2(\psi_{\sigma,\tau,\rho_2} - \text{Id}) = \tilde{P}_{\sigma,\tau,\rho_2}^2 - \text{Id}, \tag{5.3}$$

and we set

$$\psi_{\sigma,\tau,0}(z) = z + (\sigma + i\tau - |z|^2)az + \bar{z}. \tag{5.4}$$

*Remark.*  $z=0$  is always a fixed point of  $\tilde{P}_{\sigma,\tau,\rho_2}^2$  and  $\psi_{\sigma,\tau,\rho_2}$ , and  $\psi_{\sigma,\tau,0}$  possesses the symmetry of rotation by  $\pi$ .

(2) *Fixed Points of  $\tilde{P}_{\sigma,\tau,\rho_2}^2$*

As in Section IV we have the

LEMMA 5.1. *It is the same statement as Lemma 4.1, replacing  $\sigma_1, \phi_{\sigma_1,\tau,\rho}$  and  $\tilde{P}_{\sigma_1,\tau,\rho}$  by  $\rho_2, \psi_{\sigma,\tau,\rho_2}$  and  $\tilde{P}_{\sigma,\tau,\rho_2}^2$ .*

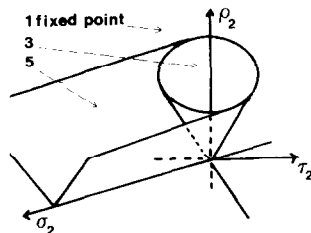


FIG. 19. Situation in the  $(\sigma_2, \tau_2, \rho_2)$  space.

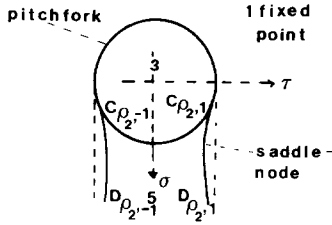


FIGURE 20

Concerning the asymptotic behavior,  $\rho_2 \rightarrow 0$ , we prove, using routine calculations as in Lemma 4.2 the

LEMMA 5.2. (1) If  $\sigma^2 + \tau^2 < 1$ ,  $\psi_{\sigma, \tau, 0}$  has three (regular) fixed points (one of them,  $z = 0$ , is a saddle point).

(2) If  $\sigma^2 + \tau^2 > 1$ ,  $|\tau| < 1$  and  $\sigma > 0$ ,  $\psi_{\sigma, \tau, 0}$  has five (regular) fixed points (two of them are saddle points).

(3) If  $\sigma^2 + \tau^2 > 1$  and  $|\tau| > 1$  or  $\sigma \leq 0$ ,  $\psi_{\sigma, \tau, 0}$  has one (regular) fixed point (which is not a saddle point).

(4) On the circle  $C_1 = \{(\sigma, \tau), \sigma^2 + \tau^2 = 1\}$ ,  $z = 0$  is the only (singular) fixed point.

(5) On the two half lines  $D_i = \{(\sigma, \tau), \sigma > 0 \text{ and } \tau = i\}$  for  $i = \pm 1$ ,  $\psi_{\sigma, \tau, 0}$  has one regular fixed point  $z = 0$  and two singular fixed points.

(Figs. 18, 19). (The fixed points are symmetric by rotation by  $\pi$ ).

Using Lemmas 5.1, 5.2 and perturbation techniques we get the

PROPOSITION 5.1. Let  $\rho_2$  be sufficiently small

(1) Inside the circle  $C_1$ ,  $\tilde{P}_{\sigma, \tau, \rho_2}^2$  possesses three (regular) fixed points (one of them,  $z = 0$ , is a saddle point). On  $C_1$ ,  $\tilde{P}_{\sigma, \tau, \rho_2}^2$  has one (singular) fixed point  $z = 0$ .

(2) There exist, on the circle  $C_1$ , two points  $C_{\rho_2, 1}$  and  $C_{\rho_2, -1}$ , defined by  $C_{\rho_2, 1} = (\cos \theta_{\rho_2, 1}, \sin \theta_{\rho_2, 1})$ ;  $C_{\rho_2, -1} = (\cos \theta_{\rho_2, -1}, \sin \theta_{\rho_2, -1})$  where  $\theta_{\rho_2, 1} = \mathcal{O}(\rho_2^{1/2})$  and  $\theta_{\rho_2, -1} = \pi + \mathcal{O}(\rho_2^{1/2})$ , such that the two new fixed points appear by pitchfork bifurcation, at  $z = 0$ , when we transversally cross  $C_1$  at  $(\cos \theta, \sin \theta)$  (Fig. 20),

from outside to inside if  $\theta_{\rho_2, 1} < \theta < \theta_{\rho_2, -1}$ ,

from inside to outside if  $\theta_{\rho_2, -1} < \theta < \theta_{\rho_2, 1} + 2\pi$ .

(3) There exist two curves  $D_{\rho_2, i}$  ( $i = -1, 1$ ), respectively defined for

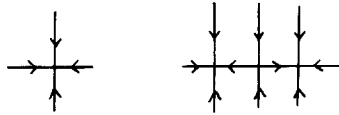


FIG. 21. A pitchfork bifurcation.

$\sigma > \sin \theta_{\rho_2, i}$ ,  $\mathcal{O}(\rho_2^{1/2})$  close to  $D_i$  ( $i = -1, 1$  and  $\sigma$  bounded), and tangent to  $C_1$  at  $C_{\rho_2, i}$  ( $i = -1, 1$ ), on which  $\tilde{P}_{\sigma, \tau, \rho_2}^2$  has a regular fixed point  $z = 0$  and two singular fixed points where saddle node bifurcations occur (Fig. 21).

(4) Let  $(\sigma, \tau)$  be outside  $C_1$

— if  $(\sigma, \tau)$  is between  $D_{\rho_2, -1}$  and  $D_{\rho_2, 1}$  (Fig. 21),  $\tilde{P}_{\sigma, \tau, \rho_2}^2$  has five fixed points (two of them are saddle points).

— if not,  $\tilde{P}_{\sigma, \tau, \rho_2}^2$  has only one fixed point  $z = 0$  which is not a saddle point.

*Remarks.* (1) The pitchfork bifurcation of  $\tilde{P}_{\sigma, \tau, \rho_2}^2$  corresponds to a flip bifurcation for the Poincaré map.

(2) In the proof of Proposition 5.1, we need to use the fact that a fixed point of  $\tilde{P}_{\sigma, \tau, \rho_2}^2$  is mapped on another fixed point by  $\tilde{P}_{\sigma, \tau, \rho_2}$ . Thanks to this, the saddle-node bifurcation points are image one of the other by  $\tilde{P}_{\sigma, \tau, \rho_2}$ , and then occur on the same curves  $D_{\rho_2, i}$ .

(3) The rescaling we have done has rejected to great values of  $\sigma$  the region where a smooth invariant circle may persist. Using the same rescaling as in Section IV we find similar results.

(2) *Sinks and Sources. Hopf Bifurcation*

We have the relation

$$\text{Det } D\tilde{P}_{\sigma, \tau, \rho_2}^2(z) = 1 + 2\rho_2 (\text{trace } D\psi_{\sigma, \tau, 0}(z) - 2) + \mathcal{O}(\rho_2^{3/2}). \quad (5.5)$$

Using similar results as in Lemma 4.3 concerning the fixed points  $z_0$  of  $\psi_{\sigma, \tau, 0}$  such that  $\text{trace } D\psi_{\sigma, \tau, 0}(z_0) = 2$ , and classical perturbation techniques we get the:

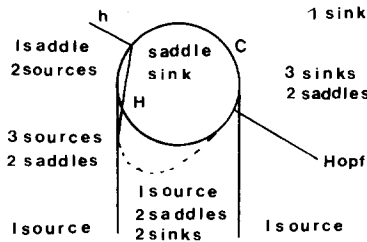


FIGURE 22

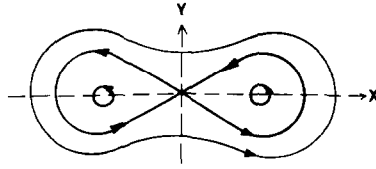


FIG. 23. The Hamiltonian system  $H_2$ .

PROPOSITION 5.2. *Let  $\rho_2$  be sufficiently small*

(1) *There exists a smooth curve  $h_{\rho_2}(\sigma, \tau) = \alpha\sigma - \beta\tau + \mathcal{O}(\rho_2^{1/2}) = 0$  on which  $\tilde{P}_{\sigma, \tau, \rho_2}$  possesses at the point  $z = 0$  a Hopf bifurcation point outside  $C_1$  and a conservative saddle point inside  $C_1$ . We denote by  $A_{\rho_2}$  and  $B_{\rho_2}$  the two intersections of  $h_{\rho_2}(\sigma, \tau) = 0$ , with the circle  $C_1$ , respectively  $\mathcal{O}(\rho_2^{1/2})$  close to  $(\beta, \alpha)$  and  $(-\beta, -\alpha)$ .*

(2) *There exists a smooth curve,  $H_{\rho_2}(\sigma, \tau) = 0, \mathcal{O}(\rho_2^{1/2})$  close to the ellipse  $(\alpha\sigma + \beta\tau)^2 + 4\alpha^2\tau^2 = 4\alpha^2$ , only defined for  $h_{\rho_2}(\sigma, \tau) \geq 0$ , containing the points  $A_{\rho_2}$  and  $B_{\rho_2}$  and tangent to  $D_{\rho_2, -1}$  at a point  $P_{\rho_2}$ , ( $\mathcal{O}(\rho_2^{1/2})$  close to  $(\beta/\alpha, -1)$ ), such that  $\tilde{P}_{\sigma, \tau, \rho_2}^2$  possesses two Hopf bifurcation points (different from zero) on the curvilinear segment  $\widehat{P_{\rho_2} B_{\rho_2}}$  and two conservative saddle points on  $\widehat{P_{\rho_2} A_{\rho_2}}$  (Fig. 22).*

We are now able to describe completely the Hopf, pitchfork and saddle-node bifurcations set in the  $(\sigma, \tau)$  space and the stability of the fixed points for small values of  $\rho_2$ .

For sake of simplicity, we represent in Fig. 22,  $D_{\rho_2, 1}, D_{\rho_2, -1}, h_{\rho_2}$  and  $H_{\rho_2}$  by their asymptotic limits. The points  $P_{\rho_2}, A_{\rho_2}$  and  $B_{\rho_2}$  correspond to fixed points with one as double non-semi-simple eigenvalue of the derivative.

(4) *Heteroclinic and Homoclinic Points*

(a) *Around the point  $P_{\rho_2}$ .* The situation is, in fact, the same as that in Section IV.4, and we can reduce the study of the Poincaré map to the

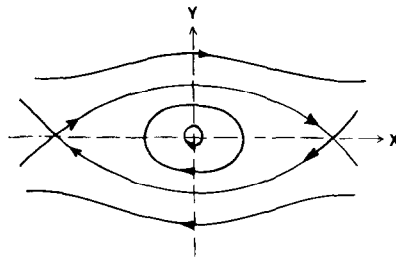


FIG. 24. The Hamiltonian system  $H_3$ .

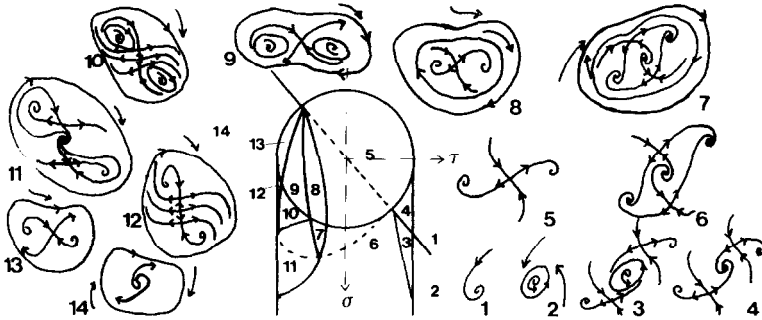


FIGURE 25

study of the perturbation of the “time  $\tau$ ” map of the Hamiltonian system  $H_1$  defined in (4.22).

(b) *Around the points  $A_{\rho_2}$  and  $B_{\rho_2}$ .* This case differs from the previous one because of the symmetry of rotation by  $\pi$ . A similar method as in Section IV.4 transforms the study of the Poincaré map in the problem of the perturbation of the “time  $\tau$ ” map of the Hamiltonian systems:

close to  $B_{\rho_2}$  (Fig. 23)

$$H_2(x, y) = y^2/2 - x^2/2 + x^4/4 \tag{5.6}$$

close to  $A_{\rho_2}$  (Fig. 24)

$$H_3(x, y) = y^2/2 + x^2/2 - x^4/4 \tag{5.7}$$

and we have, finally, the

**COROLLARY 5.1.** *Same statement as in Corollary 4.2; replacing  $n$  by  $n/2$ ,  $(n, 2) = 1$ .*

As in Section IV we give, in the following, numerical results concerning an averaging of the second iterate of the Poincaré map.

(5) *Averaging and Phase Portrait, Computer Assisted Study*

We consider the phase portrait of the differential equation which “approaches” the map  $\tilde{P}_{\sigma, \tau, \rho_2}$  (Fig. 25):

$$\frac{dz}{dt} = (\sigma + i\tau - |z|^2) az + \bar{z}. \tag{5.8}$$

*Remark.* Around  $A_0, B_0$ , in the case of ODE, a complete study has been done by Carr [3].

VI. DYNAMICS OF THE POINCARÉ MAP IN THE  $p/3$  RESONANT CASE

The dynamics of the Poincaré map is best understood if one looks at its third iterate:

$$P_{\sigma_3, \tau_3, \rho_3}^3(z) = z + 3(\sigma_3 + i\tau_3 - |z|^2)az + 3\rho_3\bar{z}^2 + \mathcal{O}(\sigma_3|z|^3) + \mathcal{O}(\tau_3|z|^3) + \mathcal{O}(\rho_3|z|^3) + \mathcal{O}(|z|^5). \quad (6.1)$$

We can reduce our study to  $\rho_3 \geq 0$  by changing  $z$  in  $e^{-i\pi/3}z$ . The fixed points different from zero of  $P_{\sigma_3, \tau_3, \rho_3}^3$  correspond to periodic points with rotation number  $p/3$ , of the Poincaré map.

(1) Rescaling

The rescaling  $z = \rho_3^{1/2}z'$ ,  $\sigma_3 + i\tau_3 = \rho_3(\sigma + i\tau)$  yields the equation (dropping primes)

$$\tilde{P}_{\sigma, \tau, \rho_3}^3(z) = z + 3\rho_3[(\sigma + i\tau - |z|^2)az + \bar{z}^2] + \mathcal{O}(\rho_3^2|z|^3). \quad (6.2)$$

The method we use now is exactly the same as the one developed in the two previous sections, and, since this strongly resonant case is the simplest one, we just sum up here the results.

(2) Fixed Points

PROPOSITION 6.1. *Let  $\rho_3$  be sufficiently small, there exists a curve  $S_{\rho_3}(\sigma, \tau) = 4\sigma + 1 - \tau^2 + \mathcal{O}(\rho_3) = 0$  such that:*

- (1) *If  $S_{\rho_3}(\sigma, \tau) < 0$ , there is only one (regular) fixed point (which is not a saddle point).*
- (2) *If  $S_{\rho_3}(\sigma, \tau) > 0$  and  $(\sigma, \tau) \neq A = (0, 0)$ ,  $\tilde{P}_{\sigma, \tau, \rho_3}^3$  has seven (regular) fixed points (three of them are saddle points).*
- (3) *If  $(\sigma, \tau) = A = (0, 0)$ , four fixed points coincide at  $z = 0$  which is a singular point, the three others are regular (not saddles).*

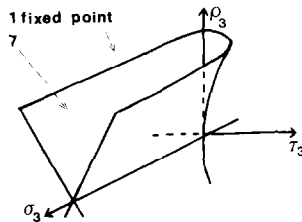


FIG. 26. Situation in the  $(\sigma_3, \tau_3, \rho_3)$  space.



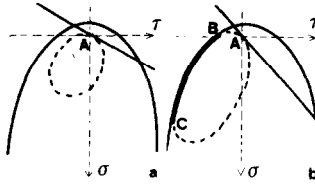


FIG. 27. Hopf and saddle-node bifurcations.  
 (a)  $\beta/\alpha < \sqrt{3}$ , (b)  $\beta/\alpha > \sqrt{3}$ .

(4) If  $S_{\rho_3}(\sigma, \tau) = 0$ ,  $\tilde{P}_{\sigma, \tau, \rho_3}^3$  has one regular fixed point  $z = 0$  and three singular fixed points (which are saddle-node bifurcation points) (Fig. 26).

(3) Sinks and Sources. Hopf Bifurcation

PROPOSITION 6.2. Let  $\rho_3$  be sufficiently small

(1) A Hopf bifurcation occurs for  $\tilde{P}_{\sigma, \tau, \rho_3}^3$  at  $z = 0$  on the line  $\alpha\sigma - \beta\tau = 0$ , except at the point  $A = (0, 0)$ .

(2) The other fixed points may have a Hopf bifurcation for

$$2\sigma + 1 + (4\sigma + 1 - 4\tau^2)^{1/2} = \sigma - \beta/\alpha + \mathcal{O}(\rho_3). \tag{6.3}$$

Equation (6.3) has solutions for any small values of  $\rho_3$  iff  $\beta/\alpha > \sqrt{3}$  (Fig. 27).

(4) Homoclinic and Heteroclinic Points

The points  $A$ ,  $B_{\rho_3}$  and  $C_{\rho_3}$  (Fig. 27) correspond to the existence of a fixed point such that 1 is a double non-semi-simple eigenvalue of its derivative.

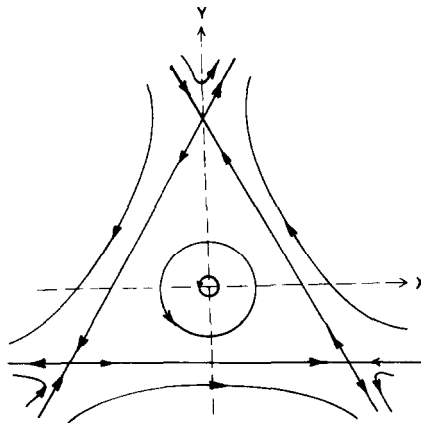


FIGURE 28

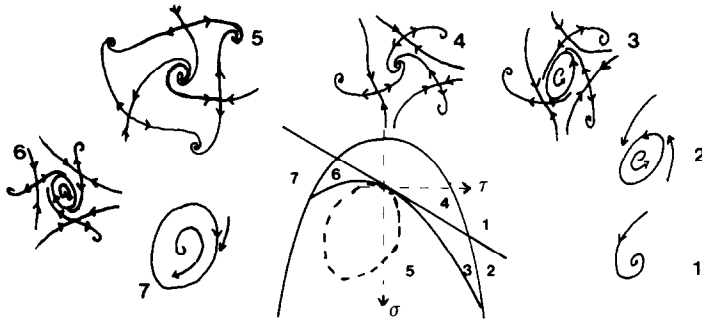


FIG. 29. Phase portrait of (6.5), in the case  $\beta/\alpha < \sqrt{3}$ .

(a) The points  $B_{\rho_3}$  and  $C_{\rho_3}$  correspond to the classical type (previously described) of the Hamiltonian  $H_1$  (4.22).

(b) Around the point  $A$ , and for  $z$  close to zero, we can reduce the study of the Poincaré map to the study of the perturbation of the “time  $\tau$  map” of the Hamiltonian (Fig. 28)

$$H_4(x, y) = x^2 + y^2 + 2x^2y - \frac{2}{3}y^3. \tag{6.4}$$

Then we have again the same results concerning homoclinic and periodic orbits:

COROLLARY 6.1. *Same statement as Corollary 4.2 changing  $n$  in  $n/3$  and  $(n, 3) = 1$ .*

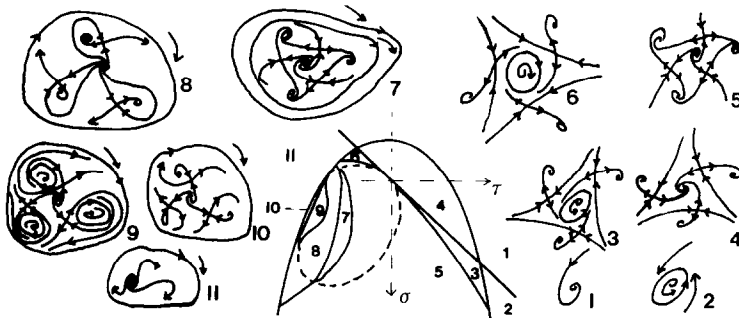


FIG. 30. Phase portrait of (6.5), in the case  $\beta/\alpha > \sqrt{3}$ .

(5) *Averaging and Phase Portraits. Computer Assisted Study*

As in the previous sections we give numerical results concerning the phase portrait of the differential equation “approaching” (in the sense defined previously)  $\tilde{P}_{\sigma, \tau, \rho_3}^3$ :

$$\frac{dz}{dt} = (\sigma + i\tau - |z|^2) az + \bar{z}^2. \quad (6.5)$$

This gives us the phase portraits (Figs. 29 and 30).

*Remark.* A detailed study has been done by Arnold [1] around the point  $A$ , in the case ODE.

## REFERENCES

1. V. ARNOLD, “Chapitres supplémentaires de la théorie des équations différentielles ordinaires,” Éditions Mir, Moscow, 1980.
2. R. BOGDANOV, Bifurcations du cycle limite d’une famille de champs de vecteurs sur le plan, *Travaux Sémin. I. Petrowski* **2** (1976) [in Russian].
3. J. CARR, “Applications of the Center Manifold Theory,” Springer-Verlag, Berlin, 1981.
4. M. L. CARTWRIGHT, Forced oscillations in nearly sinusoidal systems, *J. Inst. Elec. Engrg.* **95** (1948).
5. M. L. CARTWRIGHT, Forced oscillations in non-linear systems: Contributions to the theory of non-linear oscillations, *Ann. of Math. Stud.* **20** (1950), 149–241.
6. A. CHENCINER, Bifurcations de difféomorphismes de  $\mathbb{R}^2$  au voisinage d’un point fixe elliptique, in “Cours des Houches, 1981” (G. Iooss, R. G. Helleman, and R. Stora, Eds.), North-Holland, Amsterdam, 1983.
7. S. N. CHOW AND J. K. HALE, “Methods of Bifurcation Theory,” Springer-Verlag, Berlin, 1982.
8. J. M. GAMBAUDO, Perturbation de “l’application temps  $\tau$ ” d’un champ de vecteurs intégrable, *C. R. Acad. Sci. Paris Sér. I* **297** (1983), 245–248.
9. A. W. GILLIES, On the transformation of singularities and limit cycles of the variational equations of Van der Pol, *Quart. J. Mech. Appl. Math.* **7** (1954), 152–167.
10. P. J. HOLMES AND D. A. RAND, Bifurcations of the forced Van der Pol oscillator, *Quart. J. Math.* **35** (1978), 494–509.
11. E. HOPF, Abweigung einer periodischen losung eines Differential System, *Ber. Math. Kl. Sachs Akad. Wiss. Leipzig* **94** (1942), 1–22.
12. G. IOOSS, “Bifurcation of Maps and Applications,” Math. Studies 36, North-Holland, Amsterdam, 1979.
13. G. IOOSS, Persistence d’un cercle invariant par une application voisine de “l’application temps  $\tau$ ” d’un champ de vecteur intégrable, *C. R. Acad. Sci. Paris Sér. I* **296** (1983), 27–30, 113–116.
14. T. KAI AND K. TOMITA, Stroboscopic phase portrait of a forced non linear oscillator, *Progr. Theoret. Phys.* **61** (1979), 54–73.
15. T. KATO, “Perturbation Theory for Linear Operators,” Springer-Verlag, Berlin, 1966.

16. F. LEMAIRE, Bifurcation de Hopf pour les applications dans un cas résonnant, *C. R. Acad. Sci. Paris Sér. A* **287** (1978), 727–730.
17. D. RUELLE AND F. TAKENS, On the nature of turbulence, *Comm. Math. Phys.* **20** (1979), 167–192.
18. S. SMALE, “Diffeomorphism with Many Periodic Points, Differential and Combinatorial Topology,” Princeton Univ. Press, Princeton, N.J., 1965.